UNIVERSITY OF LEEDS

Article:
Hazanee, A, Lesnic, D orcid.org/0000-0003-3025-2770, Ismailov, MI et al. (1 more author) (2019) Inverse time-dependent source problem for the heat equation with nonlocal boundary conditions. Applied Mathematics and Computation, 346. pp. 800-815. ISSN 0096-3003

https://doi.org/10.1016/j.amc.2018.10.059

Inverse time-dependent source problems for the heat equation with nonlocal boundary conditions

A. Hazanee[a], D. Lesnic[b], M. I. Ismailov[c] and N. B. Kerimov[d]

[a] Department of Mathematics and Computer Science, Faculty of Science and Technology, Prince of Songkla University, Pattani Campus, Pattani, 94000, Thailand

[b] Department of Applied Mathematics, University of Leeds, Leeds LS2 9JT, UK

[c] Department of Mathematics, Gebze Technical University, Gebze-Kocaeli 41400, Turkey

[d] Department of Mathematics, Khazar University, Baku AZ 1096, Azerbaijan

E-mails: areena.h@psu.ac.th (A. Hazanee), amt5ld@maths.leeds.ac.uk (D. Lesnic), mismailov@gtu.edu.tr (M.I. Ismailov), nazimkerimov@yahoo.com (N.B. Kerimov).

Abstract

In this paper, we consider inverse problems of finding the time-dependent source function for the population model with population density nonlocal boundary conditions and an integral over-determination measurement. These problems arise in mathematical biology and have never been investigated in the literature in the forms proposed, although related studies do exist. The unique solvability of the inverse problems are rigorously proved using generalized Fourier series and the theory of Volterra integral equations. Continuous dependence on smooth input data also holds but, as in reality noisy errors are random and non-smooth, the inverse problems are still practically ill-posed. The degree of ill-posedness is characterised by the numerical differentiation of a noisy function. In the numerical process, the boundary element method together with either a smoothing spline regularization or the first-order Tikhonov regularization are employed with various choices of regularization parameter. One is based on the discrepancy principle and another one is the generalized cross-validation criterion. Numerical results for some benchmark test examples are presented and discussed in order to illustrate the accuracy and stability of the numerical inversion.

Keywords and phrases. Inverse source problem, Population age model, Nonlocal boundary conditions, Generalized Fourier method, Boundary element method, Regularization.

1 Introduction

Time-dependent coefficient identification problems for parabolic equations have been the point of interest for many studies, including the excellent monograph [11] and the book [16]. The time-dependent coefficient can be a free term, as in a linear inverse source problem, [4], or multiplying the dependent variable, as in a quasi-linear perfusion coefficient identification problem, [18]. The boundary conditions are usually of Dirichlet, Neumann or Robin type but, more recently, nonlocal boundary conditions arising in population age models have also been considered, [5, 6, 7]. Also, additional measurements which are sufficient to render a unique solution have been of various types, e.g. internal pointwise, boundary, integral or boundary integral, [16]. In comparison with previous related studies, [4, 6, 7, 9, 10, 12], in the current investigation, the birth rate in the population age model [15] is an arbitrary constant and the boundary conditions and the additional observation are both nonlocal and integral, respectively. One interesting point to remark is that in the case of arbitrary birth rate, the algebraic multiplicity of the auxiliary spectral problem is, in general, equal to 2 and this leads to a different treatment of generalized Fourier series analysis.

In Section 2, we formulate two new inverse time-dependent coefficient identification problems for the heat equation with nonlocal boundary conditions and integral observation. Based on rigorous proofs, their unique solvability are established in Section 3 and furthermore, continuous

dependences on smooth input data are derived. In order to add significance to our study, we allow for random errors to be considered in order to model the inherent noise present in any practical measurement. The price to pay is that the problem becomes ill-posed in the sense that any such small error in the measurement lead to highly oscillatory and unbounded errors in the output source. In order to deal with such instability regularization needs to be imposed. The boundary element method (BEM) for the numerical discretization is introduced in Section 4. Numerical results are presented and discussed in Section 5 and finally, conclusions are highlighted in Section 6.

2 Mathematical formulation

Given $T > 0$ an arbitrary fixed time of interest, consider the one-dimensional time-dependent parabolic heat equation

$$u_t(x,t) = u_{xx}(x,t) + F(x,t,u), \quad (x,t) \in \Omega_T = (0,1) \times (0,T], \tag{2.1}$$

subject to the initial condition

$$u(x,0) = \varphi(x), \quad x \in [0,1], \tag{2.2}$$

and the nonlocal boundary conditions

$$u(0,t) + bu(1,t) = 0, \quad t \in [0,T], \tag{2.3}$$

$$u_x(0,t) + u_x(1,t) = 0, \quad t \in [0,T], \tag{2.4}$$

where φ is a given function and b is a given number with $b \neq \pm 1$. Such boundary conditions arise in population age models of [15] with b representing the birth rate. More general boundary conditions of the type (2.3) and (2.4) have been considered in [6, 10]. Our goal is to determine the source term F in two cases, together with $u(x,t)$ under the additional integral measurement:

$$\int_0^1 u(x,t)\,dx = E(t), \quad t \in [0,T], \tag{2.5}$$

which represents the density of population between the ages from 0 to 1 at the moment of time t. In other diffusion applications, condition (2.5) refers to the specification of mass [2]. Related inverse problems with $b = -1$ and (2.4) replaced by the convection boundary condition

$$u_x(0,t) + \alpha u(0,t) = 0, \quad t \in [0,T], \tag{2.6}$$

where α is a Robin convection coefficient, have been considered elsewhere, [4, 7, 9, 12].

When the function F is given, the problem of finding $u(x,t)$ from the initial boundary value problem (2.1)–(2.4) is called the **direct problem**. The **inverse problem** (2.1)–(2.5) is formulated when the function F is unknown. The following two inverse problems will be studied.

The first inverse problem (IP1)

If we take the unknown function F to be $F(x,t,u) = P(t)u(x,t) + f(x,t)$, the inverse problem is formulated as the problem of finding the pair $(P(t), u(x,t))$. Then, equation (2.1) becomes

$$u_t(x,t) = u_{xx}(x,t) + P(t)u(x,t) + f(x,t), \tag{2.7}$$

where $f(x,t)$ is a given function and $P(t)$ is an unknown function. Consider the following transformation [1]:

$$v(x,t) = r(t)u(x,t), \quad r(t) = \exp\left(-\int_0^t P(\tau)\,d\tau\right). \tag{2.8}$$

Then, the inverse problem (2.2)–(2.7) transforms as

$$v_t = v_{xx} + r(t)f(x,t), \quad (x,t) \in \Omega_T, \tag{2.9}$$

$$v(x,0) = \varphi(x), \quad x \in [0,t], \tag{2.10}$$

$$v(0,t) + bv(1,t) = 0, \quad t \in [0,T], \tag{2.11}$$

$$v_x(0,t) + v_x(1,t) = 0, \quad t \in [0,T], \tag{2.12}$$

$$\int_0^1 v(x,t)dx = E(t)r(t), \quad t \in [0,T], \tag{2.13}$$

where $r(0) = 1$, $r(t) > 0$ for $t \in [0,T]$. Solving the inverse problem (2.9)–(2.13) for the solution pair $(r(t), v(x,t))$ yields afterwards the original solution $(P(t), u(x,t))$ for the inverse problem (2.2)–(2.7) from

$$P(t) = -\frac{r'(t)}{r(t)} \quad \text{and} \quad u(x,t) = \frac{v(x,t)}{r(t)}. \tag{2.14}$$

The second inverse problem (IP2)

If we take the unknown function F to be $F(x,t,u) = R(t)f(x,t)$, the inverse problem is formulated as the problem of finding the pair $(R(t), u(x,t))$ satisfying (2.2)–(2.5) and

$$u_t(x,t) = u_{xx}(x,t) + R(t)f(x,t), \tag{2.15}$$

where $f(x,t)$ is a given function and $R(t)$ is an unknown function. One can observe that the difference between IP1 given by (2.9)–(2.13) and IP2 given by (2.2)–(2.5) and (2.15), is in the different form of (2.5) compared to (2.13).

3 Mathematical analysis

In this section the eigenvalues, eigenfunctions and associated functions of the auxiliary spectral problem and some of their properties are introduced. The existence and uniqueness of the solution of inverse problem (2.2)–(2.5), (2.7) (IP1) and inverse problem (2.2)–(2.5), (2.15) (IP2) are proved. The continuous dependence upon the data of the solutions of IP1 and IP2 are also shown.

3.1 The auxiliary spectral problem

Consider the differential operator L_b generated by the differential expression $l(y) = -y''$ and boundary conditions

$$y(0) + by(1) = 0, \quad y'(0) + y'(1) = 0, \tag{3.1}$$

where b is arbitrary fixed real number.

In the case $b = -1$, the boundary conditions (3.1) are not regular whilst in the case $b \neq -1$, they are regular but not strongly regular [14]. Also, in the case $b = 1$ these boundary conditions are anti-periodic (self-adjoint). In what follows, we consider the boundary conditions (3.1) with $b \neq \pm 1$.

It is well-known that each eigenvalue of operator L_b with $b \neq \pm 1$ is of algebraic multiplicity two with one eigenfunction and one associated function corresponding to each eigenvalue.

Let the eigenvalue of operator L_b with $b \neq \pm 1$ be denoted by λ_n, $n = 1, 2, \ldots$ and the corresponding eigenfunctions and associated functions be denoted by y_{2n-1} and y_{2n}, respectively. It is easy to show that

$$\lambda_n = ((2n-1)\pi)^2, \quad y_{2n-1}(x) = \sin(\sqrt{\lambda_n}x), \quad y_{2n}(x) = \frac{b-(b-1)x}{2\sqrt{\lambda_n}(b-1)}\cos(\sqrt{\lambda_n}x), \tag{3.2}$$

for $n = 1, 2, \ldots$, such that $L_b(y_{2n-1}) = \lambda_n y_{2n-1}$ and $L_b(y_{2n}) - \lambda_n y_{2n} = y_{2n-1}$.

The adjoint differential operator L_b^* is generated by the differential expression $l^*(z) = -z''$ and boundary conditions

$$z(0) + z(1) = 0, \quad bz'(0) + z'(1) = 0. \tag{3.3}$$

The bi-orthogonal system $\{z_n(x)\}_{n=1}^{\infty}$ to the system $\{y_n(x)\}_{n=1}^{\infty}$ in the space $L_2[0,1]$ is the system of eigenfunctions $\{z_{2n}(x)\}_{n=1}^{\infty}$ and associated functions $\{z_{2n-1}(x)\}_{n=1}^{\infty}$ of operator L_b^* given by

$$z_{2n}(x) = \frac{8\sqrt{\lambda_n}(b-1)}{b+1}\cos(\sqrt{\lambda_n}x), \quad z_{2n-1}(x) = \frac{4(1+(b-1)x)}{b+1}\sin(\sqrt{\lambda_n}x), \tag{3.4}$$

for $n = 1, 2, \ldots$.

Because L_b and L_b^* are differential operators with regular boundary conditions, each of the systems $\{y_n(x)\}_{n=1}^{\infty}$ and $\{z_n(x)\}_{n=1}^{\infty}$ is complete in the space $L_2[0,1]$, [17]. Besides, it is easy to establish that for every $n \in \mathbb{N}^*$ the inequality $\|y_n\|_{L_2[0,1]} \cdot \|z_n\|_{L_2[0,1]} \leq const.$ is satisfied. From this inequality and the main result of [8], it is obtained that each of the systems $\{y_n(x)\}_{n=1}^{\infty}$ and $\{z_n(x)\}_{n=1}^{\infty}$ is an unconditional basis of the space $L_2[0,1]$.

The following lemma is obtained with the help of integration by parts and the Cauchy-Schwarz and classical Bessel inequalities.

Lemma 1. *If $\varphi(x) \in C^4[0,1]$ satisfies the conditions $\varphi(0) = \varphi''(0) = \varphi(1) = \varphi''(1) = 0$, $\varphi'(0) + \varphi'(1) = \varphi'''(0) + \varphi'''(1) = 0$, then*

$$\sum_{n=1}^{\infty} \lambda_n |\varphi_{2n}| \leq c_1 \|\varphi\|_{C^4[0,1]}, \quad \sum_{n=1}^{\infty} \lambda_n |\varphi_{2n-1}| \leq c_2 \|\varphi\|_{C^4[0,1]}, \tag{3.5}$$

for some positive constants c_1 and c_2, where $\varphi_n = \int_0^1 \varphi(x) z_n(x)\, dx$, $n = 1, 2, \ldots$.

Proof. From the assumptions on φ, the equality

$$\begin{aligned}\varphi_{2n} &= \int_0^1 \varphi(x) z_{2n}(x)\, dx = \frac{8\sqrt{\lambda_n}(b-1)}{b+1}\int_0^1 \varphi(x)\cos(\sqrt{\lambda_n}x)\, dx \\ &= \frac{8(b-1)}{\lambda_n\sqrt{\lambda_n}(b+1)}\int_0^1 \varphi^{(4)}(x)\cos(\sqrt{\lambda_n}x)\, dx,\end{aligned}$$

holds by four times integrating by parts. Analogously, by three times integrating by parts we obtain

$$\begin{aligned}\varphi_{2n-1} &= \int_0^1 \varphi(x) z_{2n-1}(x)\, dx = 4\int_0^1 \varphi(x)\left(\frac{1}{b+1} + \frac{b-1}{b+1}x\right)\sin(\sqrt{\lambda_n}x)\, dx \\ &= \frac{1}{\lambda_n\sqrt{\lambda_n}}\int_0^1 h(x)\cos(\sqrt{\lambda_n}x)\, dx,\end{aligned}$$

where $h(x) = -\frac{12(b-1)}{b+1}\varphi''(x) - 4\left(\frac{1}{b+1} + \frac{b-1}{b+1}x\right)\varphi'''(x)$.

By using the Cauchy-Schwarz and classical Bessel inequalities, we obtain

$$\begin{aligned}\sum_{n=1}^{\infty} \lambda_n |\varphi_{2n}| &\leq 8\left|\frac{b-1}{b+1}\right| \left[\sum_{n=1}^{\infty}\frac{1}{\lambda_n}\right]^{\frac{1}{2}} \left[\sum_{n=1}^{\infty}\left(\int_0^1 \varphi^{(4)}(x)\cos(\sqrt{\lambda_n}x)\, dx\right)^2\right]^{\frac{1}{2}} \\ &\leq c_1\|\varphi^{(4)}\|_{L_2[0,1]} \leq c_1\|\varphi\|_{C^4[0,1]}\end{aligned}$$

and

$$\sum_{n=1}^{\infty}\lambda_n|\varphi_{2n-1}| \le \left[\sum_{n=1}^{\infty}\frac{1}{\lambda_n}\right]^{\frac{1}{2}}\left[\sum_{n=1}^{\infty}\left(\int_0^1 h(x)\cos(\sqrt{\lambda_n}x)\,dx\right)^2\right]^{\frac{1}{2}} \le c\|h\|_{L_2[0,1]} \le c_2\|\varphi\|_{C^4[0,1]}$$

for some constants c, c_1 and c_2. □

3.2 The first inverse problem (IP1)

The pair $(P(t),u(x,t))$ from the class $C[0,T]\times\left(C^{2,1}(\Omega_T)\cap C^{1,0}(\overline{\Omega}_T)\right)$ for which conditions (2.2)–(2.5), (2.7) are satisfied, is called a classical solution of the IP1.

We consider the following assumptions on φ, E and f:

(A_1) $(A_1)_1$ $\varphi(x)\in C^4[0,1]$; $\varphi(0)=\varphi''(0)=\varphi(1)=\varphi''(1)=0$, $\varphi'(0)+\varphi'(1)=\varphi'''(0)+\varphi'''(1)=0$;
$(A_1)_2$ $\varphi_1>0$, $\varphi_n\ge 0$, $n=2,3,\dots$,

(A_2) $(A_2)_1$ $E(t)\in C^1[0,T]$; $E(0)=\int_0^1\varphi(x)\,dx$;
$(A_2)_2$ $E(t)>0$, $\forall t\in[0,T]$,

(A_3) $(A_3)_1$ $f(x,t)\in C(\overline{\Omega}_T)$; $f(\cdot,t)\in C^4[0,1]$, $f(0,t)=\frac{\partial^2 f}{\partial x^2}(0,t)=f(1,t)=\frac{\partial^2 f}{\partial x^2}(1,t)=0$, $\frac{\partial f}{\partial x}(0,t)+\frac{\partial f}{\partial x}(1,t)=\frac{\partial^3 f}{\partial x^3}(0,t)+\frac{\partial^3 f}{\partial x^3}(1,t)=0$, $\forall t\in[0,T]$;
$(A_3)_2$ $f_n(t)\ge 0$, $n=1,2,\dots$, where $f_n(t)=\int_0^1 f(x,t)z_n(x)\,dx$, $n=1,2,\dots$.

The main result of unique solvability is presented as follows.

Theorem 1. *(Existence and uniqueness of IP1)*
Let (A_1)–(A_3) be satisfied. Then the inverse problem (2.2)–(2.5), (2.7) has a unique classical solution pair $(P(t),u(x,t))$. Moreover, $u(x,t)\in C^{2,1}(\overline{\Omega}_T)$.

Proof. For arbitrary $P(t)\in C[0,T]$, we construct the formal solution of (2.2)–(2.4), (2.7) by using the generalized Fourier method. In accordance with this method, the unknown function $u(x,t)$ is sought as a Fourier series in terms of the eigenfunctions and associated functions $\{y_n(x)\}_{n=1}^{\infty}$ of the auxiliary spectral problem (3.1), as follows:

$$u(x,t)=\sum_{n=1}^{\infty}\left[u_{2n-1}(t)y_{2n-1}(x)+u_{2n}(t)y_{2n}(x)\right], \tag{3.6}$$

where the system $\{u_n(t)\}_{n=1}^{\infty}$ satisfies

$$\begin{aligned} u'_{2n}(t)&=-\lambda_n u_{2n}(t)+P(t)u_{2n}(t)+f_{2n}(t),\quad u_{2n}(0)=\varphi_{2n},\\ u'_{2n-1}(t)&=-\lambda_n u_{2n-1}(t)+P(t)u_{2n-1}(t)+u_{2n}(t)+f_{2n-1}(t),\quad u_{2n-1}(0)=\varphi_{2n-1}. \end{aligned} \tag{3.7}$$

Solving these problems, we obtain

$$\begin{aligned} u_{2n}(t)&=\varphi_{2n}e^{-\lambda_n t+\int_0^t P(s)\,ds}+\int_0^t f_{2n}(\tau)e^{-\lambda_n(t-\tau)+\int_\tau^t P(s)\,ds}\,d\tau,\\ u_{2n-1}(t)&=\varphi_{2n-1}e^{-\lambda_n t+\int_0^t P(s)\,ds}+\int_0^t\left[f_{2n-1}(\tau)+u_{2n}(\tau)\right]e^{-\lambda_n(t-\tau)+\int_\tau^t P(s)\,ds}\,d\tau\\ &=\left(\varphi_{2n-1}+t\varphi_{2n}\right)e^{-\lambda_n t+\int_0^t P(s)\,ds}\\ &\quad+\int_0^t\left[f_{2n-1}(\tau)+(t-\tau)f_{2n}(\tau)\right]e^{-\lambda_n(t-\tau)+\int_\tau^t P(s)\,ds}\,d\tau. \end{aligned} \tag{3.8}$$

Under conditions $(A_1)_1$ and $(A_3)_1$, the series (3.6), its t-partial derivative and the xx-second order partial derivative series are uniformly convergent in $\overline{\Omega}_T$ since their majorizing sums are absolutely convergent by using Lemma 1. Therefore, their sums expressing $u(x,t)$, $u_t(x,t)$ and $u_{xx}(x,t)$ are continuous in $\overline{\Omega}_T$. Thus, $u(x,t) \in C^{2,1}(\overline{\Omega}_T)$ and satisfies the conditions (2.2)–(2.4), (2.7) for arbitrary $P(t) \in C[0,T]$. Besides, the series (3.6) can be integrated term by term, and its uniqueness follows from the property of the system $\{y_n(x)\}_{n=1}^{\infty}$ being a basis of $L_2[0,1]$.

Applying the over-determination condition (2.5), we obtain the following Volterra integral equation of the second kind for $r(t)$:

$$r(t) = F(t) + \int_0^t K(t,\tau) r(\tau)\, d\tau, \quad t \in [0,T], \tag{3.9}$$

where

$$\begin{aligned} F(t) &= \frac{1}{E(t)} \sum_{n=1}^{\infty} \left[\frac{2}{\sqrt{\lambda_n}} \varphi_{2n-1} + \frac{1}{\lambda_n \sqrt{\lambda_n}} \varphi_{2n} + \frac{2t}{\sqrt{\lambda_n}} \varphi_{2n} \right] e^{-\lambda_n t}, \\ K(t,\tau) &= \frac{1}{E(t)} \sum_{n=1}^{\infty} \left[\frac{2}{\sqrt{\lambda_n}} f_{2n-1}(\tau) + \frac{1}{\lambda_n \sqrt{\lambda_n}} f_{2n}(\tau) + \frac{2(t-\tau)}{\sqrt{\lambda_n}} f_{2n}(\tau) \right] e^{-\lambda_n (t-\tau)}, \end{aligned} \tag{3.10}$$

where we have used that

$$\int_0^1 y_{2n}(x)\, dx = \frac{1}{\lambda_n \sqrt{\lambda_n}}, \quad \int_0^1 y_{2n-1}(x)\, dx = \frac{2}{\sqrt{\lambda_n}}. \tag{3.11}$$

In the case of existence of a positive solution of (3.9) in class $C^1[0,T]$ satisfying $r(0) = 1$, the function $P(t)$ can be determined from (2.14).

By using Lemma 1, under assumptions $(A_1)_1$, $(A_2)_1$ and $(A_3)_1$, the right-hand side $F(t)$ and the kernel $K(t,\tau)$ are continuously differentiable functions in $[0,T]$ and $[0,T]\times[0,T]$, respectively. In addition, according to assumptions $(A_1)_2$, $(A_2)_2$ and $(A_3)_2$, conditions $F(t) > 0$ and $K(t,\tau) \geq 0$ are satisfied in $[0,T]$ and $[0,T] \times [0,T]$, respectively.

From the theory of Volterra integral equations of the second kind we obtain that (3.9) has a unique positive solution $r(t)$, continuously differentiable in $[0,T]$, satisfying

$$r(0) = F(0) = \frac{1}{E(0)} \sum_{n=1}^{\infty} \frac{1}{\sqrt{\lambda_n}} \left[2\varphi_{2n-1} + \frac{1}{\lambda_n} \varphi_{2n} \right] = 1, \tag{3.12}$$

where, in deriving (3.12), we have used (3.6) at $t = 0$ integrated with respect to x from 0 to 1 and $(A_2)_1$. □

Remark 1. To see that assumptions $(A_1) - (A_3)$ can indeed be satisfied, we give a simple example, as follows. Let T and b be arbitrary positive numbers and take the input data

$$\varphi(x) = \sin(\pi x), \quad f(x,t) = \pi^2 \sin(\pi x) e^{\chi(t)}, \quad E(t) = 2e^{\chi(t)}/\pi,$$

where $\chi \in C^1[0,T]$ is an arbitrary function. It can easily be checked that this data satisfy $(A_1) - (A_3)$. Then, according to Theorem 1 it follows that the IP1 given by (2.2)-(2.5), (2.7) has a unique solution, which can be verified to be

$$P(t) = \chi'(t), \quad u(x,t) = \sin(\pi x) e^{\chi(t)}. \tag{3.13}$$

Also, as performed in Section 2, the transformation (2.8) yields the problem (2.9)-(2.13), which has the unique solution

$$r(t) = e^{\chi(0) - \chi(t)}, \quad v(x,t) = \sin(\pi x) e^{\chi(0)}. \tag{3.14}$$

The following result on the continuous dependence on the data of the solution of IP1 holds.

Theorem 2. *(Continuous dependence upon the data for IP1)*
Let $\mathfrak{T}$ be the class of triples in the form of $\{f, \varphi, E\}$ which satisfy the assumptions (A_1)–(A_3) and

$$\|f\|_{C^{4,0}(\overline{\Omega}_T)} \le N_0, \quad \|\varphi\|_{C^4[0,1]} \le N_1, \quad \|E\|_{C^1[0,T]} \le N_2, \quad 0 < N_3 \le \min_{t\in[0,T]} |E(t)|, \tag{3.15}$$

for some given positive constants N_i, $i = 0, 1, 2, 3$. Then the solution pair (P, u) of the inverse problem (2.2)–(2.5), (2.7) depends continuously upon the data in $\mathfrak{T}$.

The proof of this theorem is omitted since it is very similar to that of Theorem 4 of [13].

3.3 The second inverse problem (IP2)

The pair $(R(t), u(x,t))$ from the class $C[0,T] \times \left(C^{2,1}(\Omega_T) \cap C^{1,0}(\overline{\Omega})\right)$ for which conditions (2.2)–(2.5), (2.15) are satisfied, is called a classical solution of the IP2.

The main result of unique solvability is presented as follows.

Theorem 3. *(Existence and uniqueness of IP2)*
Let $(A_1)_1$, $(A_2)_1$ and $(A_3)_1$ be satisfied. Assume also that $\int_0^1 f(x,t)\,dx \neq 0$, $\forall t \in [0,T]$. Then the inverse problem (2.2)–(2.5), (2.15) has a unique classical solution pair $(R(t), u(x,t))$. Moreover, $u(x,t) \in C^{2,1}(\overline{\Omega}_T)$.

Proof. By applying the standard procedure of the Fourier method, we obtain the following representation for the solution of (2.2)–(2.4), (2.15) for arbitrary $R(t) \in C[0,T]$:

$$u(x,t) = \sum_{n=1}^{\infty} \left[v_{2n-1}(t) y_{2n-1}(x) + v_{2n}(t) y_{2n}(x)\right], \tag{3.16}$$

where

$$\begin{aligned} v_{2n}(t) &= \varphi_{2n} e^{-\lambda_n t} + \int_0^t R(\tau) f_{2n}(\tau) e^{-\lambda_n (t-\tau)}\,d\tau, \\ v_{2n-1}(t) &= \varphi_{2n-1} e^{-\lambda_n t} + t\varphi_{2n} e^{-\lambda_n t} + \int_0^t R(\tau)\left[f_{2n-1}(\tau) + (t-\tau) f_{2n}(\tau)\right] e^{-\lambda_n (t-\tau)}\,d\tau. \end{aligned} \tag{3.17}$$

Under assumptions $(A_1)_1$ and $(A_3)_1$, the series (3.16), its t-partial and the xx-partial derivatives are uniformly convergent in $\overline{\Omega}_T$ since their majorizing sums are absolutely convergent by using Lemma 1. Therefore, their sums expressing $u(x,t)$, $u_t(x,t)$ and $u_{xx}(x,t)$ are continuous in $\overline{\Omega}_T$. Thus, $u(x,t) \in C^{2,1}(\overline{\Omega}_T)$ and satisfies the conditions (2.2)–(2.4) and (2.15) for an arbitrary $R(t) \in C[0,T]$. Besides, the series (3.16) can be integrated term by term, and its uniqueness follows from the property of the system $\{y_n(x)\}_{n=1}^{\infty}$ being a basis of $L_2[0,1]$.

Equations (2.5) and (3.16) yield the following Volterra integral equation of the first kind with respect to $R(t)$:

$$\int_0^t \tilde{K}(t,\tau) R(\tau)\,d\tau + \tilde{F}(t) = E(t), \quad t \in [0,T], \tag{3.18}$$

where

$$\tilde{F}(t) = F(t)E(t), \quad \tilde{K}(t,\tau) = K(t,\tau)E(t). \tag{3.19}$$

By using Lemma 1, under the assumptions of Theorem 3, the term $\tilde{F}(t)$ and the kernel $\tilde{K}(t,\tau)$ are continuously differentiable functions in $[0,T]$ and $[0,T] \times [0,T]$, respectively. It is easy to show that

$$\tilde{K}(t,t) = \sum_{n=1}^{\infty} \left[\frac{2}{\sqrt{\lambda_n}} f_{2n-1}(t) + \frac{1}{\lambda_n \sqrt{\lambda_n}} f_{2n}(t)\right] = \int_0^1 f(x,t)\,dx,$$

since

$$f(x,t)=\sum_{n=1}^{\infty}\left[f_{2n-1}(t)y_{2n-1}(x)+f_{2n}(t)y_{2n}(x)\right].$$

Further, under assumption $(A_2)_1$, equation (3.18) yields the following Volterra integral equation of the second kind:

$$\tilde{K}(t,t)R(t)+\int_0^t \tilde{K}_t(t,\tau)R(\tau)\,d\tau+\tilde{F}'(t)=E'(t),\quad t\in[0,T]. \tag{3.20}$$

Note that function $\tilde{K}(t,t)$ is never equal to zero because of the assumption $\int_0^1 f(x,t)\,dx\neq 0$, $\forall t\in[0,T]$. In addition, the functions $\tilde{F}'(t)$, $E'(t)$ and the kernel $\tilde{K}_t(t,\tau)$ are continuous functions in $[0,T]$ and $[0,T]\times[0,T]$, respectively. As in the previous section, from the theory of Volterra integral equations of the second kind, we obtain a unique function $R(t)$, continuous on $[0,T]$, which, together with (3.16), form the unique solution of IP2. □

The following result on continuously dependence on the data of the solution of the IP2 holds.

Theorem 4. *(Continuous dependence upon the data for IP2)*
Let $\mathfrak{F}$ be the class of triples in the form of $\{f,\varphi,E\}$ which satisfy assumptions $(A_1)_1$, $(A_2)_1$ and $(A_3)_1$, and

$$\|f\|_{C^{4,0}(\overline{\Omega}_T)}\leq M_0,\quad \|\varphi\|_{C^4[0,1]}\leq M_1,\quad \|E\|_{C^1[0,T]}\leq M_2,\quad 0<M_3\leq\left|\int_0^1 f(x,t)\,dx\right|, \tag{3.21}$$

for some given positive constants M_i, $i=0,1,2,3$. Then the solution pair (R,u) of the inverse problem (2.2)–(2.5), (2.15) depends continuously upon the data in $\mathfrak{F}$.

The proof of this theorem is omitted since it is similar to that of Theorem 2 of [5].

Theorems 1 and 2 in fact establish that the IP1 under investigation given by equations (2.2)–(2.5), (2.7) is well-posed in appropriate spaces of regular functions. The same situation is also true from Theorems 3 and 4 which establish that the IP2 given by equations (2.2)–(2.5), (2.15) is well-posed. However, in practice the input data, especially the measured one, such as the density/energy/mass (2.5), is non-smooth and hence, the solution of the inverse problem becomes unstable under unregularised noisy differentiation (see also expression (2.14)).

The next section describes the discretization of the inverse problem using the boundary element method (BEM), whilst Section 5 will present and discuss the numerical results.

4 Boundary Element Method (BEM)

In this section, we present the BEM based on using the fundamental solution for the heat equation, to discretise the two inverse problems (2.9)–(2.13) and (2.2)–(2.5), (2.15) for IP1 and IP2, respectively. In addition to the well-known advantages over full domain discretisation methods, such as the finite-difference or the finite element methods, the BEM employed in this section does not require any time marching procedure and thus, the imposition of the additional condition (2.5) can be performed globally on the full time interval $[0,T]$.

4.1 BEM for IP1

We first consider the case of IP1 consisting of finding the pair solution $(r(t),v(x,t))$ which, via expression (2.8), leads to the original solution pair $(P(t),u(x,t))$. Let us introduce the fundamental solution G of the one-dimensional parabolic heat equation defined as

$$G(x,t;y,\tau)=\frac{H(t-\tau)}{\sqrt{4\pi(t-\tau)}}\exp\left(-\frac{(x-y)^2}{4(t-\tau)}\right),$$

where H is the Heaviside step function. Using this fundamental solution and the Green's formula, equation (2.9) can be written in the following boundary integral form, see e.g. [3]:

$$\begin{aligned}
&\eta(x)v(x,t)\\
&= \int_0^t \left(G(x,t;\xi,\tau)\frac{\partial v}{\partial n(\xi)}(\xi,\tau) - v(\xi,\tau)\frac{\partial G}{\partial n(\xi)}(x,t;\xi,\tau)\right)\Bigg|_{\xi\in\{0,1\}} d\tau + \int_0^1 G(x,t;y,0)v(y,0)\,dy\\
&\quad + \int_0^1\int_0^T G(x,t,y,\tau)r(\tau)f(y,\tau)\,d\tau dy, \quad (x,t)\in[0,1]\times(0,T],
\end{aligned} \tag{4.1}$$

where $\eta(0)=\eta(1)=0.5$, $\eta(x)=1$ for $x\in(0,1)$, and $\underline{n}$ is the outward unit normal to the space boundary $\{0,1\}$. For discretising (4.1), we divide the boundaries $\{0\}\times[0,T]$ and $\{L\}\times[0,T]$ into N small time-intervals $[t_{j-1},t_j]$, $j=\overline{1,N}$, with $t_j=\frac{jT}{N}$, $j=\overline{0,N}$, whilst the initial domain $[0,L]\times\{0\}$ is divided into N_0 small cells $[x_{k-1},x_k]$, $k=\overline{1,N_0}$ with $x_k=\frac{k}{N_0}$, $k=\overline{0,N_0}$. Over each boundary element, the transformed solutions v and $\frac{\partial v}{\partial n}$ are assumed to be constant and take their values at the midpoint $\tilde{t}_j=\dfrac{t_{j-1}+t_j}{2}$, i.e.

$$\begin{aligned}
&v(0,t)=v(0,\tilde{t}_j)=:h_{0j}, \quad v(1,t)=v(1,\tilde{t}_j)=:h_{1j},\\
&\frac{\partial v}{\partial n}(0,t)=\frac{\partial v}{\partial n}(0,\tilde{t}_j)=:q_{0j}, \quad \frac{\partial v}{\partial n}(1,t)=\frac{\partial v}{\partial n}(1,\tilde{t}_j)=:q_{1j},
\end{aligned}$$

for $t\in(t_{j-1},t_j]$. Similarly, in each cell, the initial population $v(x,0)$ is assumed to be constant and takes its value at the midpoint $\tilde{x}_k=\dfrac{x_{k-1}+x_k}{2}$, i.e.

$$v(x,0)=\varphi(x)=\varphi(\tilde{x}_k)=:\varphi_k \quad \text{for} \quad x\in[x_{k-1},x_k).$$

For the source term, the functions $f(x,t)$ and $r(t)$ are approximated to be the piecewise constant functions

$$f(x,t)=f(x,\tilde{t}_j), \quad r(t)=r(\tilde{t}_j)=:r_j, \quad \text{for} \quad t\in(t_{j-1},t_j].$$

Applying the boundary conditions (2.11) and (2.12), with the above piecewise constant BEM approximations, the boundary integral equation (4.1) becomes

$$\begin{aligned}
\eta(x)v(x,t) =& \sum_{j=1}^{N}\left(-A_{0j}(x,t)q_{1j}+A_{1j}(x,t)q_{1j}+bB_{0j}(x,t)h_{1j}-B_{1j}(x,t)h_{1j}\right)\\
&+\sum_{k=1}^{N_0}C_k(x,t)\varphi_k+\sum_{j=1}^{N}D_j(x,t)r_j,
\end{aligned} \tag{4.2}$$

where the coefficients are given by

$$\begin{aligned}
&A_{\xi j}(x,t)=\int_{t_{j-1}}^{t_j}G(x,t;\xi,\tau)d\tau, \quad B_{\xi j}(x,t)=\int_{t_{j-1}}^{t_j}\frac{\partial G}{\partial n}(x,t;\xi,\tau)d\tau, \quad \xi\in[0,1],\\
&C_k(x,t)=\int_{x_{k-1}}^{x_k}G(x,t;y,0)\,dy, \quad D_j(x,t)=\int_0^1 f(y,\tilde{t}_j)A_{yi}(x,t)\,dy,
\end{aligned}$$

for $j=\overline{1,N}$, $k=\overline{1,N_0}$. The integrals $A_{\xi j}(x,t)$, $B_{\xi j}(x,t)$ and $C_k(x,t)$ can be evaluated analytically, [3, 4], whilst Simpson's rule is used as a numerical integration for calculating the integral

$D_j(x,t)$. Applying (4.2) at the boundary nodes $(0,\tilde{t}_i)$ and $(1,\tilde{t}_i)$ for $i=\overline{1,N}$ yields the system of $2N$ linear equations

$$-A_0\underline{\mathrm{q}}_1+A_1\underline{\mathrm{q}}_1+bB_0\underline{\mathrm{h}}_1-B_1\underline{\mathrm{h}}_1+C\underline{\varphi}+D\underline{\mathrm{r}}=\underline{0}, \tag{4.3}$$

where

$$\begin{aligned}
&A_0=\begin{bmatrix}A_{0j}(0,\tilde{t}_i)\\A_{0j}(1,\tilde{t}_i)\end{bmatrix}_{2N\times N}, && A_1=\begin{bmatrix}A_{1j}(0,\tilde{t}_i)\\A_{1j}(1,\tilde{t}_i)\end{bmatrix}_{2N\times N},\\
&B_0=\begin{bmatrix}B_{0j}(0,\tilde{t}_i)+\frac{1}{2}\delta_{ij}\\B_{0j}(1,\tilde{t}_i)\end{bmatrix}_{2N\times N}, && B_1=\begin{bmatrix}B_{1j}(0,\tilde{t}_i)\\B_{1j}(1,\tilde{t}_i)+\frac{1}{2}\delta_{ij}\end{bmatrix}_{2N\times N},\\
&C=\begin{bmatrix}C_k(0,\tilde{t}_i)\\C_k(1,\tilde{t}_i)\end{bmatrix}_{2N\times N_0}, && D=\begin{bmatrix}D_j(0,\tilde{t}_i)\\D_j(1,\tilde{t}_i)\end{bmatrix}_{2N\times N},\\
&\underline{\mathrm{q}}_1=\left[q_{1j}\right]_N, \quad \underline{\mathrm{h}}_1=\left[h_{1j}\right]_N, && \underline{\varphi}=\left[\varphi_k\right]_{N_0}, \quad \underline{\mathrm{r}}=\left[r_j\right]_N,
\end{aligned}$$

and δ_{ij} is the Kronecker delta symbol. The system of equations (4.3) can be rewritten as

$$\begin{bmatrix}\underline{\mathrm{q}}_1\\\underline{\mathrm{h}}_1\end{bmatrix}=\Big[(A_0-A_1)\Big|(-bB_0+B_1)\Big]^{-1}\left[C\underline{\varphi}+D\underline{\mathrm{r}}\right], \tag{4.4}$$

where $\Big[(A_0-A_1)\Big|(-bB_0+B_1)\Big]$ is a $2N\times 2N$ matrix formed with the $2N\times N$ block matrices (A_0-A_1) and $(-bB_0+B_1)$ separated by the vertical line.

Next, we collocate the additional condition (2.13) by using the midpoint numerical integration approximation at the discrete time $\tilde{t}_i$ for $i=\overline{1,N}$, as

$$e_ir_i:=E(\tilde{t}_i)r(\tilde{t}_i)=\int_0^1 v(x,\tilde{t}_i)\,dx=\frac{1}{N_0}\sum_{k=1}^{N_0}v(\tilde{x}_k,\tilde{t}_i), \quad i=\overline{1,N}. \tag{4.5}$$

Then, expression (4.5), via (4.2) applied at $(\tilde{x}_k,\tilde{t}_i)$, yields

$$\frac{1}{N_0}\sum_{k=1}^{N_0}\left(-A_{0,k}^{(1)}\underline{\mathrm{q}}_1+A_{1,k}^{(1)}\underline{\mathrm{q}}_1+bB_{0,k}^{(1)}\underline{\mathrm{h}}_1-B_{1,k}^{(1)}\underline{\mathrm{h}}_1+C_k^{(1)}\underline{\varphi}+D_k^{(1)}\underline{\mathrm{r}}\right)=E\underline{\mathrm{r}}, \tag{4.6}$$

where

$$\begin{aligned}
&A_{0,k}^{(1)}=\left[A_{0j}(\tilde{x}_k,\tilde{t}_i)\right]_{N\times N}, \quad A_{1,k}^{(1)}=\left[A_{1j}(\tilde{x}_k,\tilde{t}_i)\right]_{N\times N},\\
&B_{0,k}^{(1)}=\left[B_{0j}(\tilde{x}_k,\tilde{t}_i)\right]_{N\times N}, \quad B_{1,k}^{(1)}=\left[B_{1j}(\tilde{x}_k,\tilde{t}_i)\right]_{N\times N},\\
&C_k^{(1)}=\left[C_l(\tilde{x}_k,\tilde{t}_i)\right]_{N\times N_0}, \quad D_k^{(1)}=\left[D_j(\tilde{x}_k,\tilde{t}_i)\right]_{N\times N},\\
&E=\operatorname{diag}(e_1,\ldots,e_N), \quad k,l=\overline{1,N_0}, \quad i,j=\overline{1,N}.
\end{aligned}$$

Expression (4.6) can be also rewritten as

$$\frac{1}{N_0}\sum_{k=1}^{N_0}\left(\Big[(-A_{0,k}^{(1)}+A_{1,k}^{(1)})\Big|(bB_{0,k}^{(1)}-B_{1,k}^{(1)})\Big]\begin{bmatrix}\underline{\mathrm{q}}_1\\\underline{\mathrm{h}}_1\end{bmatrix}+C_k^{(1)}\underline{\varphi}+D_k^{(1)}\underline{\mathrm{r}}\right)=E\underline{\mathrm{r}}. \tag{4.7}$$

Eliminating $\underline{\mathrm{q}}_1$ and $\underline{\mathrm{h}}_1$ by substituting (4.4) into (4.7), the unknown function $\underline{\mathrm{r}}$ can be found by solving the $N\times N$ linear system of equations

$$X_1\underline{\mathrm{r}}=\underline{\mathrm{y}}_1, \tag{4.8}$$

where

$$X_1 = E - \frac{1}{N_0}\sum_{k=1}^{N_0}\left(\left[(-A_{0,k}^{(1)} + A_{1,k}^{(1)})\Big|(bB_{0,k}^{(1)} - B_{1,k}^{(1)})\right]\left[(A_0 - A_1)\Big|(-bB_0 + B_1)\right]^{-1} D + D_k^{(1)}\right),$$

$$\underline{\mathrm{y}}_1 = \frac{1}{N_0}\sum_{k=1}^{N_0}\left(\left[(-A_{0,k}^{(1)} + A_{1,k}^{(1)})\Big|(bB_{0,k}^{(1)} - B_{1,k}^{(1)})\right]\left[(A_0 - A_1)\Big|(-bB_0 + B_1)\right]^{-1} C + C_k^{(1)}\right)\underline{\varphi}.$$

4.2 BEM for IP2

In this subsection, we consider the BEM for solving the inverse problem (2.2)–(2.5), (2.15). As before, we obtain (as in (4.3))

$$-A_0\underline{\mathrm{q}}_1 + A_1\underline{\mathrm{q}}_1 + bB_0\underline{\mathrm{h}}_1 - B_1\underline{\mathrm{h}}_1 + C\underline{\varphi} + D\underline{\mathrm{R}} = \underline{0}. \tag{4.9}$$

For the integral over-determination condition (2.5), the midpoint numerical integration is utilized to obtain

$$e_i := E(\tilde{t}_i) = \int_0^1 u(x,\tilde{t}_i)\,dx = \frac{1}{N_0}\sum_{k=1}^{N_0} u(\tilde{x}_k,\tilde{t}_i), \quad i = \overline{1,N}. \tag{4.10}$$

By the BEM procedure that we have described earlier, applying the above integral approximation condition yields

$$\frac{1}{N_0}\sum_{k=1}^{N_0}\left(\left[(-A_{0,k}^{(1)} + A_{1,k}^{(1)})\Big|(bB_{0,k}^{(1)} - B_{1,k}^{(1)})\right]\begin{bmatrix}\underline{\mathrm{q}}_1\\ \underline{\mathrm{h}}_1\end{bmatrix} + C_k^{(1)}\underline{\varphi} + D_k^{(1)}\underline{\mathrm{R}}\right) = \underline{\mathrm{e}}, \tag{4.11}$$

where $\underline{\mathrm{e}} = \left[e_i\right]_N$. Eliminating $\underline{\mathrm{h}}_{1j}$ and $\underline{\mathrm{q}}_{1j}$ between (4.9) and (4.11), we obtain the system of $N \times N$ linear equations

$$X_2\underline{\mathrm{R}} = \underline{\mathrm{y}}_2, \tag{4.12}$$

where

$$X_2 = \frac{1}{N_0}\sum_{k=1}^{N_0}\left(\left[(-A_{0,k}^{(1)} + A_{1,k}^{(1)})\Big|(bB_{0,k}^{(1)} - B_{1,k}^{(1)})\right]\left[(A_0 - A_1)\Big|(-bB_0 + B_1)\right]^{-1} D + D_k^{(1)}\right),$$

$$\underline{\mathrm{y}}_2 = \underline{\mathrm{e}} - \frac{1}{N_0}\sum_{k=1}^{N_0}\left(\left[(-A_{0,k}^{(1)} + A_{1,k}^{(1)})\Big|(bB_{0,k}^{(1)} - B_{1,k}^{(1)})\right]\left[(A_0 - A_1)\Big|(-bB_0 + B_1)\right]^{-1} C + C_k^{(1)}\right)\underline{\varphi}.$$

5 Numerical results and discussion

This section presents two typical test examples for the identification of time-dependent smooth and non-smooth continuous source functions in order to test the accuracy of the BEM numerical procedure introduced earlier in Section 4. The following root mean square error (RMSE) is used to evaluate the accuracy of the numerical results:

$$\mathrm{RMSE} = \sqrt{\frac{T}{N}\sum_{i=1}^{N}\big(Exact(\tilde{t}_i) - Approximate(\tilde{t}_i)\big)^2}. \tag{5.1}$$

5.1 Example 1 (IP1)

In this example, we consider the inverse problem IP1 given by (2.2)–(2.5), (2.7) which, via (2.8), can be transformed into the inverse problem (2.9)–(2.13). This example is considered for the identification of the time-dependent coefficient $P(t)$ and the population $u(x,t)$ given by

$$P(t) = 1 + t, \quad u(x,t) = x^4(1-x)^3 e^{t+t^2/2}, \tag{5.2}$$

whilst the analytical solution for the transformed problem (2.9)–(2.13) is

$$r(t) = e^{-(t+t^2/2)}, \quad v(x,t) = x^4(1-x)^3.$$

The input data is

$$\varphi(x) = x^4(1-x)^3, \quad f(x,t) = 6x^2(x-1)(7x^2-8x+2)e^{t+t^2/2}, \quad E(t) = \frac{1}{280}e^{t+t^2/2},$$

and we take $T = 1$ and $b = 2$. This input data satisfy almost all the assumptions of Theorem 1, except for some of the $(A_1)_2$. Nevertheless, the solution (5.2) does exist, and although its uniqueness cannot strictly be inferred from Theorem 1, the computations below indicate that this is indeed the case.

As we have mentioned before, the original solution pair $(P(t), u(x,t))$ can be calculated from $(r(t), v(x,t))$ using (2.14).

We start by considering the linear BEM system of equations (4.8). The normalized singular values of matrix X_1 in (4.8) for $N = N_0 \in \{20, 40, 80\}$ are shown in Figure 1 with the corresponding condition numbers 4.173, 4.322 and 4.399, respectively. The singular values and the condition number of the matrix X_1 have been calculated using the Matlab commands svd(X_1) and cond(X_1), respectively. From these condition numbers it can be seen that the linear system of equations (4.8) is well-conditioned, indicating that the inverse problem (2.9)–(2.13) for finding the solution pair $(r(t), u(x,t))$ is well-posed.

Next, we consider the numerical test with $N = N_0 = 40$ as these numbers of boundary elements and cells were found to be sufficiently large to ensure that any further increase in this discretization did not significantly affect the accuracy of the numerical solutions.

For exact data, Figure 2 shows an excellent agreement between the exact solution and the numerical solution obtained directly using the inversion of (4.8), i.e. $\underline{\mathrm{r}} = X_1^{-1}\underline{\mathrm{y}}_1$, based on a Gaussian elimination method implemented in Matlab using the command gaussElim($X_1, \underline{\mathrm{y}}_1$). As the corresponding curves are virtually undistinguishable, for more clarity, we report the RMSE values (5.1) given by RMSE(r) = 4.9E-5, RMSE(r') = 7.3E-3, RMSE(P) = 1.9E-2 and RMSE($u(0,\cdot)$) = 3.9E-6. To obtain $P(t)$ and $u(0,t)$, we use (2.14) with the derivative $r'(t)$ calculated using the finite-difference formulae,

$$r'(\tilde{t}_1) = \frac{r(\tilde{t}_1) - 1}{T/(2N)}, \quad r'(\tilde{t}_i) = \frac{r(\tilde{t}_i) - r(\tilde{t}_{i-1})}{T/N}, \quad i = \overline{2, N}. \tag{5.3}$$

In practice, the contamination of measured data by unplanned error is unavoidable. Thus we add noise to the input data $E(t)$ in (2.5) in order to test the stability of the solution. The input data $\underline{\mathrm{E}}^\epsilon$ is perturbed by random Gaussian additive noise as

$$\underline{\mathrm{E}}^\epsilon = \underline{\mathrm{E}} + \underline{\epsilon}, \tag{5.4}$$

where $\underline{\epsilon} = random('\mathrm{Normal}', 0, \sigma, N, 1)$ is a set of N variables generated randomly by the MATLAB command for a normal distribution with the zero mean and standard deviation σ given by

$$\sigma = p \times \max_{t\in[0,T]} |E(t)|, \tag{5.5}$$

and p is the percentage of noise. For Example 1, the maximum value of the input data $E(t)$ is $\max_{t\in[0,T]}|E(t)| = e/3$, so that the standard deviation is $\sigma = ep/3$. This perturbation implies that the matrix X_1 in (4.8) is contaminated with noise and is denoted by X_1^ϵ. Then, when noise is present, instead of solving (4.8), we have to solve the noisy system of linear equations $X_1^\epsilon \underline{\mathrm{r}} = \underline{\mathrm{y}}_1$. Figure 2 displays in dash-dot line $(-\cdot-)$ the numerical results with $p = 1\%$ noisy input for $r(t)$, $r'(t)$, $P(t)$ and $u(0,t)$, obtained by using the straightforward inversion of the perturbed BEM linear system,

$$\underline{\mathrm{r}}^\epsilon = (X_1^\epsilon)^{-1}\underline{\mathrm{y}}_1. \tag{5.6}$$

From this figure, it can be seen clearly that the numerical results for $r(t)$ and $u(0,t)$ are relatively accurate but the numerical results for $r'(t)$ and $P(t)$ are highly oscillatory and unbounded because the numerical differentiation of a noisy function is an unstable procedure.

In order to overcome this instability, we employ the smoothing spline technique introduced in [20] which is a regularization method for differentiating a noisy function. In this method, we approximate the noisy data $(r(\tilde{t}_j))_{j=\overline{1,N}}$ by the smoothed function $\hat{r} \in C^1(\mathbb{R})$ with $\hat{r}'' \in L^2(\mathbb{R})$, which minimizes the second-order Tikhonov regularization function, [7, 20]

$$\mathcal{I}_\Lambda(\hat{r}) := \frac{T}{N}\sum_{j=1}^{N}(\hat{r}(\tilde{t}_j) - r_j^\epsilon)^2 + \Lambda\|\hat{r}''\|^2_{L^2(\mathbb{R})}, \tag{5.7}$$

where $\Lambda \geq 0$ is a regularization parameter to be prescribed and r_j^ϵ is the noisy approximate solution (5.6) obtained by direct inversion without regularization. This smoothed function $\hat{r}$ can be approximated by the cubic spline

$$\hat{r}(t) = d_1 + d_2 t + \sum_{j=1}^{N} c_j|t - \tilde{t}_j|^3, \tag{5.8}$$

where $\{c_j\}_{j=\overline{1,N}}$ and $\{d_j\}_{j=\overline{1,2}}$ are unknown constant coefficients to be determined by inserting (5.8) into (5.7) and minimizing the resulting expression with respect to these coefficients. This yields the following system of $N+2$ equations with $N+2$ unknowns, [20],

$$\hat{r}_\Lambda(\tilde{t}_j) + \frac{12\Lambda N c_j}{T} = r_j^\epsilon, \quad j = \overline{1,N}, \tag{5.9}$$

$$\sum_{j=1}^{N} c_j = \sum_{j=1}^{N} c_j\tilde{t}_j = 0, \tag{5.10}$$

where $\hat{r}_\Lambda$ denotes the numerical solution obtained using the regularization parameter Λ. By solving the system of linear equations (5.9) and (5.10) we obtain the coefficients $\{c_j\}_{i=\overline{1,N}}$ and $\{d_j\}_{j=\overline{1,2}}$ and therefore the smooth function $\hat{r}$. By differentiating this function with respect to t, we obtain the first-order derivative $r'(t)$ given by

$$\hat{r}'(t) = d_2 + 3\sum_{j=1}^{N} c_j(t - \tilde{t}_j)^2\mathrm{sign}(t - \tilde{t}_j), \tag{5.11}$$

where $\mathrm{sign}(\cdot)$ is the signum function. From (5.9), one can observe that if $\Lambda = 0$ then $\hat{\underline{\mathrm{r}}}_0 = \underline{\mathrm{r}}^\epsilon$. Therefore, in the case of exact data actually one can take $\Lambda = 0$, as the numerical results obtained using the straightforward inversion are stable and accurate, as illustrated in Figure 2. But for noisy data, taking $\Lambda = 0$ produces highly unbounded and oscillatory solutions for $r'(t)$ and $P(t)$, as shown in Figure 2 by the dash-dot line $(-\cdot-)$. Wei and Li [20] suggested two choices for the regularization parameter Λ. One is the *a priori* choice defined by

$$\Lambda = \frac{T}{N}\|\underline{\mathrm{r}} - \underline{\mathrm{r}}^\epsilon\|^2 =: \kappa, \tag{5.12}$$

where $\underline{r}$ is the exact solution. The other one is the discrepancy principle based on the *a posteriori* choice of Λ satisfying

$$\frac{T}{N}\|\hat{\underline{r}}_\Lambda - \underline{r}^\epsilon\|^2 \approx \kappa. \tag{5.13}$$

For $p = 1\%$ noise, the *a priori* and a *a posteriori* choices (5.12) and (5.13) yield $\Lambda_\kappa = 3.2E-4$ and $\Lambda_{dis} = 1.4E-4$, respectively.

Figure 3 displays the numerical results for $r'(t)$ and $P(t)$ obtained by using the BEM together with the smoothing spline regularization with Λ_κ and Λ_{dis}. It is clear to see that the numerical results obtained by both the *a priori* and *a posteriori* choices of regularization parameters are stable and more accurate than the results without the regularization (Figure 2). Also, the *a posteriori* choice (5.13) is slightly more accurate then the *a priori* choice (5.12).

5.2 Example 2 (IP2)

In the previous example, we have considered the inverse problem of finding the time-dependent coefficient $P(t)$ in the IP1 by using the BEM together with the smoothing spline regularization technique. In this example, we are considering the time-dependent source identification function $R(t)$ in IP2 by using the BEM together with the Tikhonov regularization. We consider a severe test example of finding a discontinuous source function given by [21],

$$R(t) = \begin{cases} -1, & t \in [0, 0.2), \\ 1, & t \in [0.25, 0.5), \\ -1, & t \in [0.5, 0.75), \\ 1, & t \in [0.75, 1], \end{cases} \tag{5.14}$$

with the input data $T = 1$, $b = 2$, $\varphi(x) = 0$ and $f(x,t) = 1$. In this case, as there is no analytical solution available for the direct problem, the data $E(t)$ is not available either. However, we can simulate the data (2.5) numerically by solving first the direct problem (2.2)–(2.4), (2.15), with R known and given by (5.14). The numerical results for $u(0,t)$, $u_x(0,t)$ and $E(t)$ obtained by using the BEM with various numbers of elements and cells $N = N_0 \in \{20, 40, 80\}$ are shown in Figure 4. From this figure it can be seen that the numerical solution is convergent as the number of boundary elements increases, in addition there is little difference between the numerical results obtained with the various mesh sizes showing that the independence of the mesh has been achieved.

We start by considering the linear BEM system of equations (4.12). The normalized singular values of matrix X_2 for $N = N_0 \in \{20, 40, 80\}$ are shown in Figure 1 with the corresponding condition numbers 290.6, 905.9 and 2736.7, respectively. In contrast with the singular values and low condition numbers of the matrix X_1 for IP1, the low singular values and large condition numbers of the matrix X_2 for IP2 indicate that the linear system of equations (4.12) is ill-conditioned, hence the inverse problem (2.2)-(2.5), (2.15) for finding the solution pair $(R(t), u(x,t))$ is ill-posed.

We then take the numerical result for $E(t)$ in Figure 4 simulated from the direct problem with $N = N_0 = 40$, as the input data in (2.5) in the inverse problem (2.2)-(2.5), (2.15). In order to avoid committing an inverse crime, the number of boundary elements is kept to be the same $N = 40$, but the number of cells is taken as $N_0 = 30$ to be different from 40 which was used in the direct problem.

For exact data, the numerical results for $r(t)$, $u(0,t)$ and $u_x(0,t)$ obtained by solving the inverse problem (2.2)–(2.5), (2.15) with the BEM for $N = 40$, $N_0 = 30$ are illustrated in Figure 5. These results have been obtained using the straightforward inversion of the linear system of equations (4.12), i.e. $\underline{R} = X_2^{-1}\underline{y}_2$. The very good agreement between the analytical and numerical results is observed, with no Gibbs corner phenomenon manifested.

Next, the input data (2.5) is perturbed by $p = 1\%$ random Gaussian additive noise calculated by (5.4) with the standard deviation given by (5.5). The numerical solutions shown in Figure 5 by a dash-dot line $(-\cdot-)$ have been obtained with no regularization, i.e. using the straightforward inversion of the noisy linear system, namely,

$$\underline{\mathrm{R}}^{\epsilon} = X_2^{-1}\underline{\mathrm{y}}_2^{\epsilon}. \tag{5.15}$$

From this figure it can be seen that the numerical solution for $R(t)$ is unstable, however, the results for $u(0,t)$ and $u_x(0,t)$ seem to remain stable. This is somewhat to be expected since the triplet solution $(R(t), u(0,t), u_x(0,t))$ of IP2 is stable in the components of $u(0,t)$ and $u_x(0,t)$, but unstable in the source function $R(t)$.

In order to overcome this instability, we employ the first-order Tikhonov regularization given by

$$\underline{\mathrm{r}}_{\lambda} = \left(X_2^{\mathrm{T}}X_2 + \lambda\mathcal{R}\right)^{-1} X_2^{\mathrm{T}}\underline{\mathrm{y}}_2^{\epsilon}, \tag{5.16}$$

where $\lambda > 0$ is a regularization parameter to be prescribed and $\mathcal{R}$ is corresponding to the first-order differential regularization matrix given by [19],

$$\mathcal{R} = \begin{bmatrix} 1 & -1 & 0 & 0 & . \\ -1 & 2 & -1 & 0 & . \\ 0 & -1 & 2 & -1 & . \\ . & . & . & . & . \end{bmatrix}. \tag{5.17}$$

Note that the case of using the straightforward inversion (5.15) is equivalent to the case of no regularization, i.e. $\lambda = 0$, and of the use of Gaussian elimination technique. For choosing the regularization parameter, we use the generalised cross-validation (GCV) criterion. This method is a popular choice of the regularization parameter which is based on minimising the GCV function, [21],

$$GCV(\lambda) = \frac{\|X_2\left(X_2^{\mathrm{T}}X_2 + \lambda\mathcal{R}\right)^{-1}X_2^{\mathrm{T}}\underline{\mathrm{y}}_2^{\epsilon} - \underline{\mathrm{y}}_2^{\epsilon}\|^2}{\left[\mathrm{trace}(I - X_2(X_2^{\mathrm{T}}X_2 + \lambda\mathcal{R})^{-1}X_2^{\mathrm{T}})\right]^2}. \tag{5.18}$$

The numerically obtained results presented in Figure 6 and Table 1 illustrate that stable and accurate solutions have been obtained.

6 Conclusions

Two new inverse problems of finding the time-dependent source term in a parabolic equation, with nonlocal boundary conditions and an integral observation, have been investigated. The first inverse problem has been transformed to an inverse source problem with an unknown term existing in the integral over-determination condition. The existence, uniqueness, and continuous dependence upon the data of the classical solution of the inverse problems have been rigorously established. The significance of the study has been enhanced by inverting overspecified data contaminated with noise in order to model the errors which are always present in any practical measurement. The numerical discretization was based on the BEM combined with either the smoothing spline regularization for IP1, or the first-order Tikhonov regularization for IP2. In the case of the transformed problem IP1, *a priori* and *a posteriori* choices of regularization parameters have been investigated, whilst the GCV criterion has been employed for IP2. The numerical results have been found accurate and stable. Future work will concern multi-dimensional extensions of the current mathematical and numerical analyses.

References

[1] Cannon, J.R., Lin, Y. and Wang, S. (1991) Determination of a control parameter in a parabolic partial differential equation, *Journal of the Australian Mathematical Society, Series B* **33**, 149-163.

[2] Cannon, J.R. and van der Hoek, J. (1986) Diffusion subject to the specification of mass, *Journal of Mathematical Analysis and Applications* **115**, 517-529.

[3] Farcas, A. and Lesnic, D. (2006) The boundary element method for the determination of a heat source dependent on one variable, *Journal of Engineering Mathematics* **54**, 375-388.

[4] Hazanee, A., Ismailov, M.I., Lesnic, D. and Kerimov, N.B. (2013) An inverse time-dependent source problem for the heat equation, *Applied Numerical Mathematics* **69**, 13-33.

[5] Hazanee, A., Ismailov, M.I., Lesnic, D. and Kerimov, N.B. (2015) An inverse time-dependent source problem for the heat equation with a non-classical boundary condition, *Applied Mathematical Modelling* **39**, 6258-6272.

[6] Hazanee, A. and Lesnic, D. (2013) Determination of a time-dependent heat source from nonlocal boundary conditions, *Engineering Analysis with Boundary Elements* **37**, 936-956.

[7] Hazanee, A. and Lesnic, D. (2014) Determination of a time-dependent coefficient in the bioheat equation, *International Journal of Mechanical Sciences* **88**, 259-266.

[8] Ilin, V.A. (1983) Unconditional basis property on a closed interval of systems of eigenvalues and associated functions of a second-order differential operator, *Doklady Akademii Nauk SSSR* **273**, 1048-1053.

[9] Ismailov, M.I., Kanca, F. and Lesnic, D. (2011) Determination of a time-dependent heat source under nonlocal boundary and integral overdetermination conditions, *Applied Mathematics and Computation* **218**, 4138-4146.

[10] Ivanchov, N.I. (1995) On the determination of unknown source in the heat equation with nonlocal boundary conditions, *Ukrainian Mathematical Journal* **47**, 1647-1652.

[11] Ivanchov, M.I. (2003) *Inverse Problems for Equations of Parabolic Type*, VNTL Publications, Lviv, Ukraine.

[12] Kerimov, N.B. and Ismailov, M.I. (2012) An inverse coefficient problem for the heat equation in the case of nonlocal boundary conditions, *Journal of Mathematical Analysis and Applications* **396**, 546-554.

[13] Kerimov, N.B. and Ismailov, M.I. (2015) Direct and inverse problems for the heat equation with a dynamic-type boundary conditions, *IMA Journal of Applied Mathematics* **80**, 1519-1533.

[14] Naimark, M.A. (1967) *Linear Differential Operators: Elementary Theory of Linear Differential Operators*, Frederick Ungar Publishing Co., New York.

[15] Nakhushev, A.M. (1985) *Equations of Mathematical Biology*, Vysshaya Shkola, Moscow, (in Russian).

[16] Prilepko, A.I., Orlovski, D.G. and Vasin, I.A. (2000) *Methods for Solving Inverse Problems in Mathematical Physics*, Marcel Dekker, New York.

[17] Shkalikov, A.A. (1982) Bases formed by eigenfunctions of ordinary differential operators with integral boundary conditions, *Vestnik Moskovskogo Universiteta Seriya I Matematika Mekhanika* **120**, 12-21.

[18] Trucu, D., Ingham, D.B. and Lesnic, D. (2008) Inverse time-dependent perfusion coefficient identification, *Journal of Physics: Conference Series* **124**, 012050 (28 pages).

[19] Twomey, S. (1963) On the numerical solution of Fredholm integral equations of the first kind by the inversion of the linear system produced by quadrature, *Journal of the Association for Computing Machinery* **10**, 97-101.

[20] Wei, T. and Li, M. (2006) High order numerical derivatives for one-dimensional scattered noisy data, *Applied Mathematics and Computation* **175**, 1744-1759.

[21] Yan, L., Fu, C.L. and Yang, F.L. (2008) The method of fundamental solutions for the inverse heat source problem, *Engineering Analysis with Boundary Elements* **32**, 216-222.

Table 1: The values of λ_{GCV} and RMSEs for $r(t)$, $u(0,t)$ and $u_x(0,t)$ obtained using the BEM together with the first-order Tikhonov regularization and $p \in \{0,1,3,5\}\%$ noise, for $N = 40$, $N_0 = 30$, for Example 2.

p	λ	$r(t)$	$u(0,t)$	$u_x(0,t)$
$p = 0\%$	$\lambda = 0$	1.420E-3	7.663E-5	2.554E-4
$p = 1\%$	$\lambda = 0$	7.361E-1	8.526E-3	6.138E-2
$p = 1\%$	λ_{GCV} =1.4E-5	1.760E-1	7.088E-3	4.017E-2
$p = 3\%$	λ_{GCV} =1.8E-4	2.268E-1	1.376E-2	6.518E-2
$p = 5\%$	λ_{GCV} =1.0E-3	3.048E-1	2.478E-2	1.139E-1

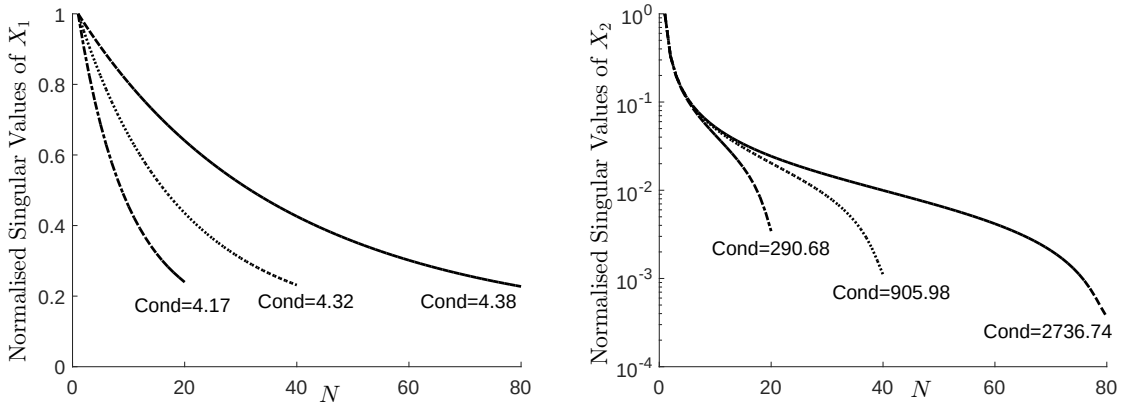

Figure 1: The normalized singular values of matrix X_1 for Example 1 and of matrix X_2 for Example 2, for $N = N_0 \in \{20\,(- \cdot -),\ 40\,(\cdots),\ 80\,(- - -)\}$.

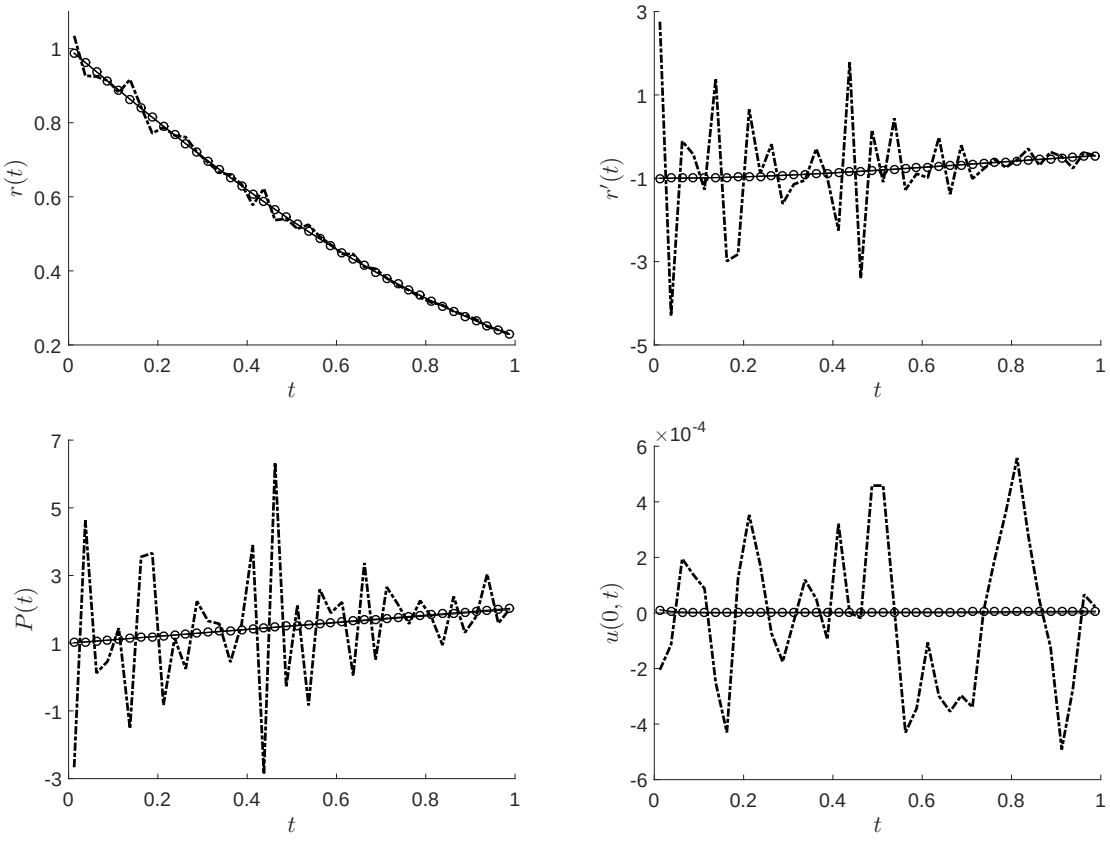

Figure 2: The analytical (—) and numerical results of $r(t)$, $r'(t)$, $P(t)$ and $u(0,t)$ for exact data ($\circ\circ\circ$), i.e. $p = 0$, and $p = 1\%$ ($- \cdot -$) noisy data, with no regularization, for Example 1.

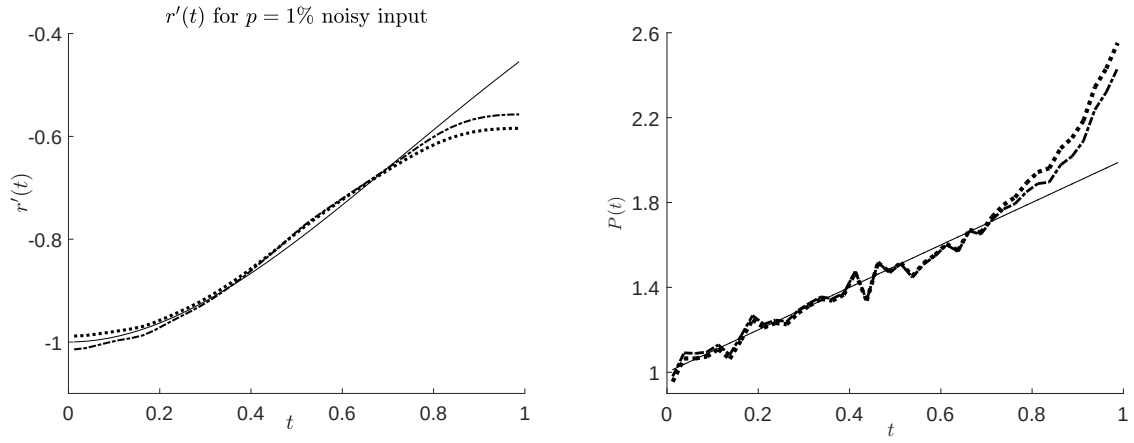

Figure 3: The analytical (——) and numerical results of $r'(t)$ and $P(t)$ obtained using the smoothing spline regularization with $\Lambda_\kappa = 3.2E-4$ $(\cdots)$ and $\Lambda_{dis} = 1.4E-4$ $(-\cdot-)$ for $p = 1\%$ noisy data, for Example 1.

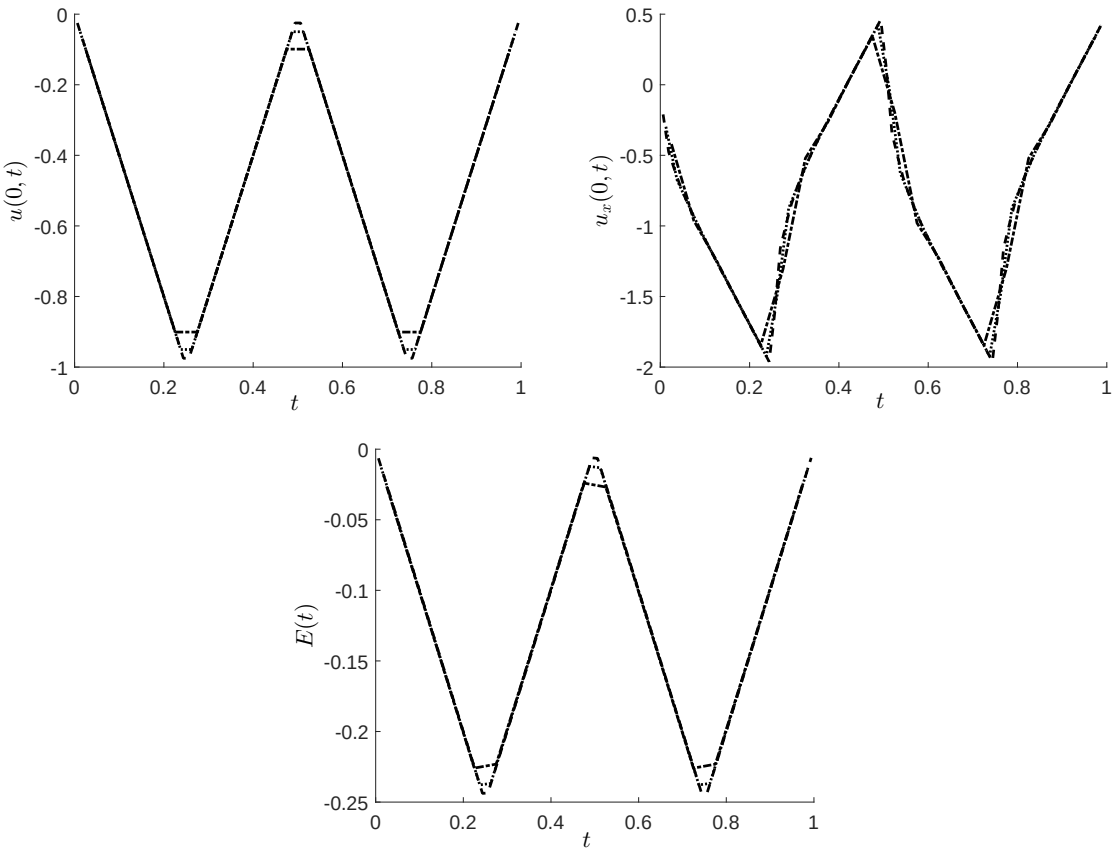

Figure 4: The numerical results of $u(0,t)$, $u_x(0,t)$ and $E(t)$ obtained by solving the direct problem (2.2)–(2.4), (2.15) using the BEM with $N = N_0 = \{20\,(- \cdot -),\ 40\,(\cdots),\ 80\,(- - -)\}$, for Example 2.

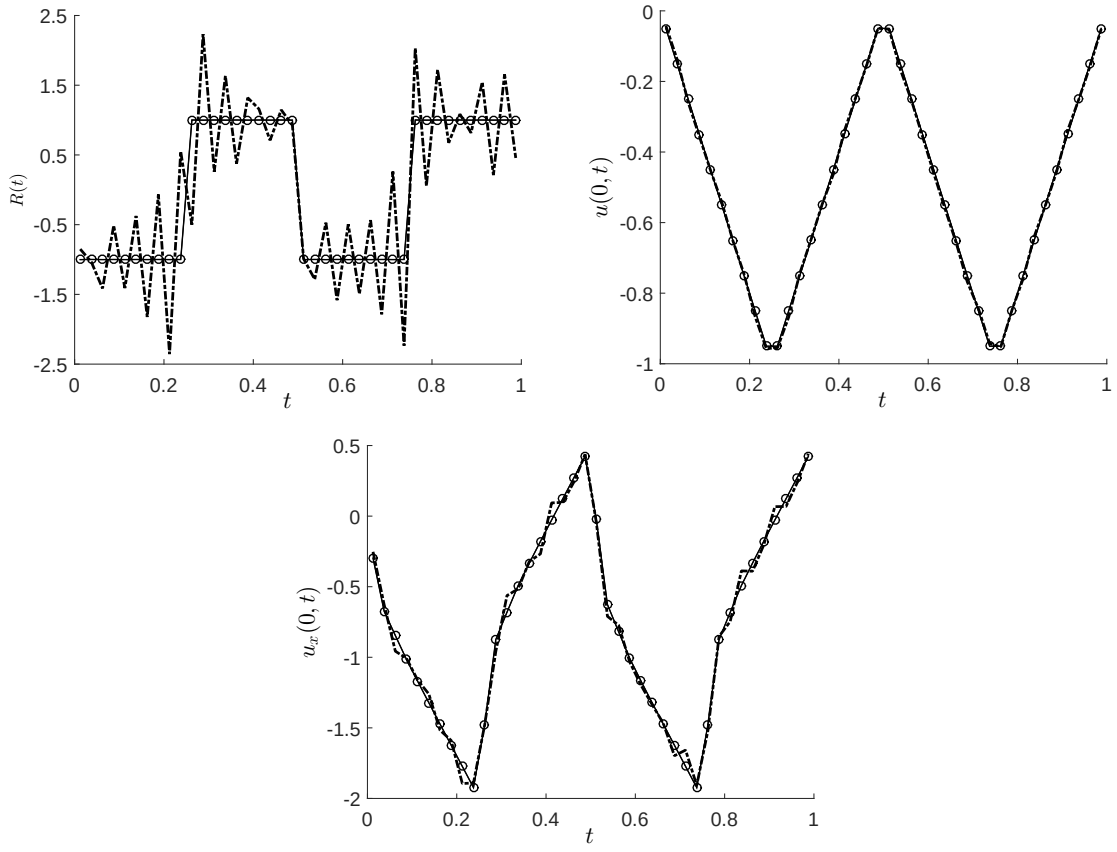

Figure 5: The analytical (—) and numerical results of $r(t)$, $u(0,t)$ and $u_x(0,t)$ for exact data ($\circ\circ\circ$) and $p = 1\%$ noise ($-\cdot-$), with no regularization ($\lambda = 0$), for Example 2.

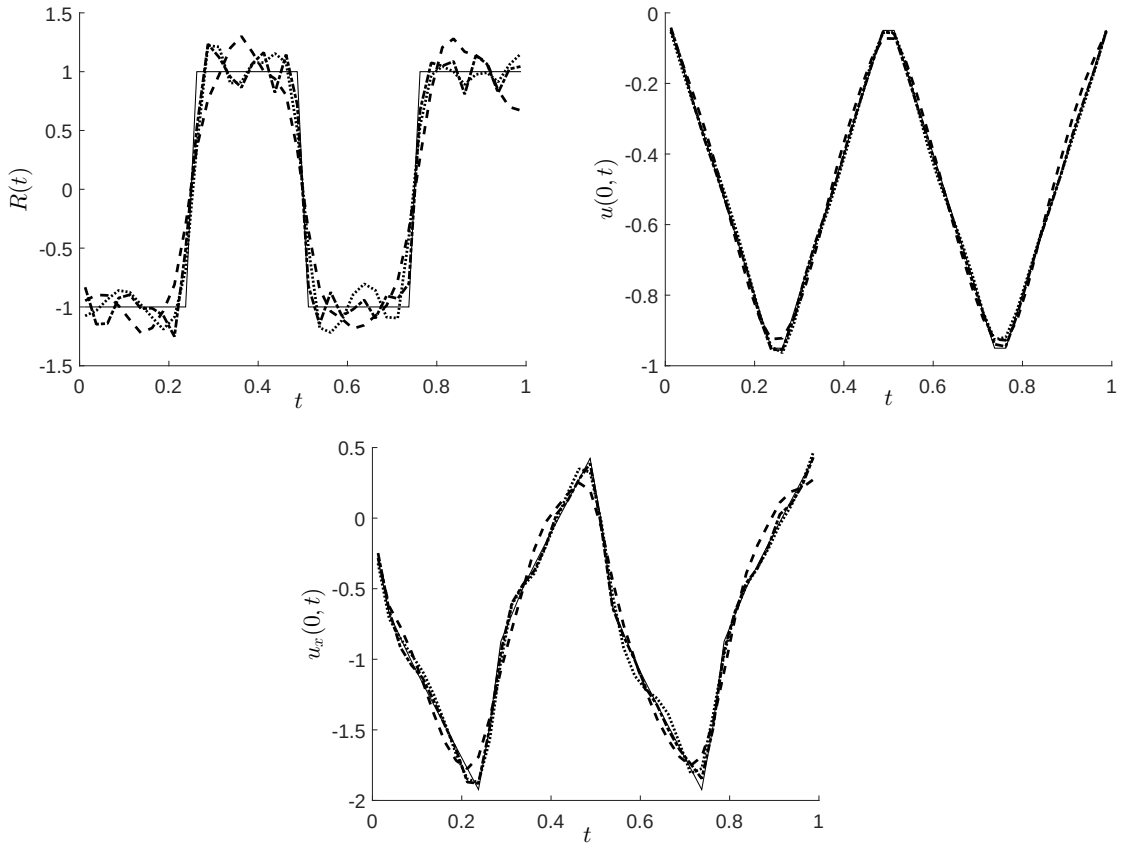

Figure 6: The analytical (—) and numerical results of $r(t)$, $u(0,t)$ and $u_x(0,t)$ obtained using the first-order Tikhonov regularization for $p \in \{1(- \cdot -),\ 3(\cdots),\ 5(- - -)\}\%$ noisy data with the regularization parameter $\lambda_{GCV} \in \{1.4\text{E-}5, 1.8\text{E-}4, 1.0\text{E-}3\}$, respectively, for Example 2.